Proceedings of the 28th IEEE
EMBS Annual International Conference
New York City, USA, Aug 30-Sept 3, 2006

Generalized Series Solution for the Induced E-Field Distribution of Slinky-type Magnetic Stimulators

Marcílio Feitosa, *Member IEEE* and Eduardo Fontana

Abstract— **Magnetic stimulation is a technique to excite biological tissues by means of a time-varying magnetic field. This induced electric field can depolarize the cell membrane so as to evoke an action potential that propagates along neurons, eventually being transmitted to other neurons or to a muscular cell. Design of a magnetic stimulator requires modeling of the impulse propagation along the nerve cell, as well as numerical simulations for coil design optimization to determine adequate excitation levels as well as the degree of focalization on a given target cell. In this paper we report on a new methodology to calculate the stimulation field for the case of the traditional slinky coil geometry, that greatly reduces computation time, thus facilitating simulation studies of the dynamics of electric impulse propagation along a nerve cell.**

I. INTRODUCTION

ARTIFICIAL nervous stimulation is a technique that has become very important to physicians and researchers in the medical field. It assists in diagnosis and treatment of certain types of nervous system disorders [1]. Electric stimulation of the nervous system using electrodes has a wide range of applications, especially in physiotherapy. On the other hand, magnetic stimulation of the nervous system has benefits not provided by the conventional electrode method. The method consists of stimulating tissues by means of an electric field induced by a time-varying magnetic field. The main benefit for using this approach is that the magnetic field penetrates easily in deep and electrically insulated tissues of the body, such as those found in bones and fat [1]-[2].

Design of a magnetic stimulator comprises modeling of the dynamics of electric propagation along a nerve fiber, so as to establish minimum stimulation levels as well as coil design studies for adequate focalization of the stimulation field and achievement of the minimum stimulation level determined from the dynamic model.

This work was supported in part by the Programa de Demanda Social, CAPES, and by CNPq, Project No. 302710/2003-5

Marcílio A. F. Feitosa, *IEEE Eng. Med. Biol. Soc* member, is with the Grupo de Fotônica, Departamento de Eletrônica e Sistemas, Universidade Federal de Pernambuco, Recife, PE 50.740-530, Brazil, Phone: +55-81-21268210,+55-81-21268995, Fax +55-81-21268215 (e-mail: marciliofeitosa@uol.com.br).

Eduardo Fontana is with the Grupo de Fotônica, Departamento de Eletrônica e Sistemas, Universidade Federal de Pernambuco, Recife, PE 50.740-530, Brazil, Phone: +55-81-21268210,+55-81-21268995, Fax +55-81-21268215 (e-mail: fontana@ufpe.br).

II. DYNAMIC MODEL OF THE AXON MEMBRANE

The dynamics of propagation of an electric disturbance through neurons or nerve fibers can be made with the help of the so-called Hodgkin-Huxley model [3], in which the axon, i.e., the nervous fiber through which the action potential propagates, is modeled as a distributed parameter transmission line, as depicted in Fig.1 The equivalent transmission line in this model has shunt conductances, g_{Na}, g_K, and g_L related to the ionic channels for sodium, potassium and other ions, respectively, and those are non-linear functions of the membrane voltage [3]. The membrane wall is modeled electrically as a capacitor, having a capacitance per unit length c_m, as depicted in Fig.2, and the ionic solution within the axon is represented electrically by a series resistor having a resistance per unit length r_i. The active ionic channels (that produce an ionic gradient between membrane faces) are represented by the voltage sources E_{Na}, E_K, and E_L, associated with the ionic gradient across the membrane faces for Na, K and other ions, respectively.

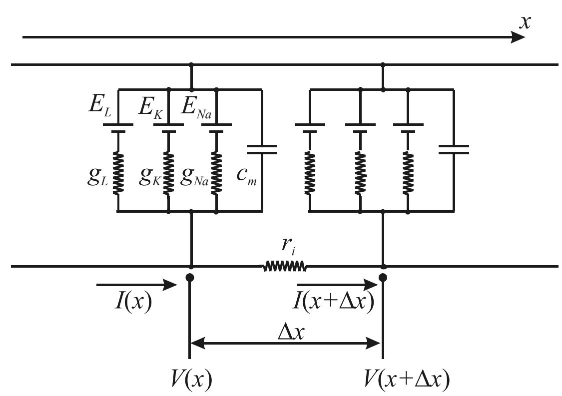

Fig.1. Distributed parameter model of the axon membrane.

For the case of an axon directed along the x direction, submitted to a magnetically induced electric field E_x, the action potential V across the membrane satisfies the differential equation

$$\Lambda^2 \frac{\partial^2 V}{\partial x^2} - V = \tau \frac{\partial V}{\partial t} + \Lambda^2 \frac{\partial E_x}{\partial x} \tag{1}$$

where the space and time constants in (1) are given by

$$\Lambda^2 = \frac{r_m}{r_i}, \tag{2}$$

1-4244-0033-3/06/$20.00 ©2006 IEEE.

and $$\tau = r_m c_m\,, \tag{3}$$

with r_m representing the equivalent shunt resistance in the model, which is a non-linear function of the membrane action potential V, through the shunt conductance, as well as the active voltage sources depicted in Fig.1. One can notice that (1) has in principle a diffusion type structure due to the second derivative in space and first derivative in time. In fact, if the stimulation field has a level below a certain threshold, any voltage disturbance produced at a point only diffuses longitudinally, causing only small deviation of the equilibrium membrane voltage, without any propagation. There is a threshold value of stimulus, however, above which the action potential propagates as an undumped wave, the velocity of which depending on the intrinsic nerve parameters [4].

III. Design Issues

As (1) indicates, the dominant term under magnetic stimulation is the x-derivative of the x-component of the external electric field, a parameter that depends on the coil geometry of the stimulator. A number of investigators have employed circular coils for developing magnetic stimulators [5]. Others have proposed the slinky coil geometry depicted in Fig.2, as a route to decrease the lateral spread of the stimulation field, so as to minimize the effects of an undesired magnetic stimulation of other nerves on the body [6]. We have showed in a previous study that for the butterfly shaped geometry depicted in Fig.2, and for a stationary apex relative to the work surface, one can reach a minimum relative *rms* width of the stimulating field gradient for an angle of approximately 47 deg between the coil plane and the working surface. Our calculations also revealed that the butterfly-shaped design at the optimum angular position concentrated the field gradient within a region about 65% that of the conventional circular coil [7]

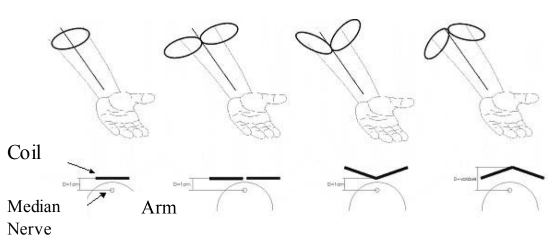

Fig. 2. A classical circular coil and a slinky coil for fixed and variable apex positions.

In an effort to determining an optimum slinky geometry from joint coil design and dynamic simulation studies, we have found that the conventional integral formulation for calculation of the induced E-field introduced a long time delay in the numerical simulations of the action potential dynamics. Because of this we have developed an analytical expression for the induced E-field, as well as the space derivative used as input in (1), valid for any number of loops and sizes in the coil geometry. We verified that using this approach computation time was reduced at least 10 times, relative to that within the integral formulation. This model is described next.

IV. Theoretical Model

We consider the determination of the induced electric field due to N circular loops, with the k-th loop having a radius r_k and carrying a current i_k, as shown in Fig.3. All loops have a single common point at the origin of the xyz system and the plane of each loop is located on a plane that is rotated relative to the xy plane about the x axis. Within the quasi-static approximation, the electric field induced by the current carrying loops is given by [8]

$$\vec{E} = -\frac{\partial \vec{A}}{\partial t} \tag{4}$$

with $\vec{A}$ representing the vector potential, that can be written in the form

$$\vec{A} = \frac{\mu_0}{4}\sum_{k=1}^{N} i_k F_k\left(R_k, u_k\right)\hat{a}_{\phi k} \tag{5}$$

with

$$F_k = \int_0^{2\pi} \frac{r_k \cos\phi d\phi}{\left|R_k \hat{a}_{Rk} - r_k \hat{a}_{r'k}\right|}\,, \tag{6}$$

with r_k representing the radius of the k-th loop that carries a time varying current i_k, and

$$\hat{a}_{r'k} = \cos\phi \hat{a}_{rk} + \sin\phi \hat{a}_{\phi k} \tag{7}$$

representing a variable vector along the radial direction deviated ϕ radians from the fixed radial direction defined by the cylindrical unit vector $\hat{a}_{rk}$, and R_k, representing the radial distance in spherical coordinates form the loop center. From (5) one can obtain (4) and the stimulation term appearing in the RHS of (1).

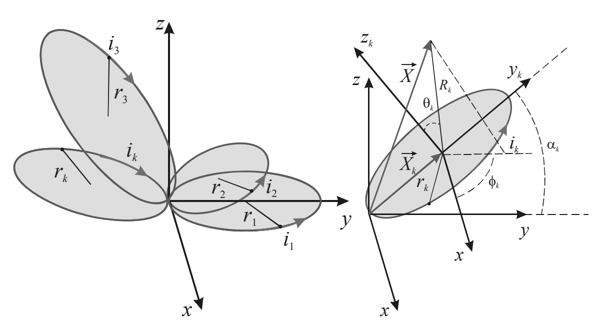

(a) (b)

Fig.3. (a) Slinky coil geometry. (b) Reference frame for the k-th loop.

We can show that the stimulation term can be written as

$$\frac{\partial E_x}{\partial x} = -x\frac{\mu_0}{4}\sum_{k=1}^{N}\frac{di_k}{dt}\frac{r_k\left(y\cos\alpha_k + z\sin\alpha_k - r_k\right)H_k}{R_k^2\left(1-u_k^2\right)} \quad (8)$$

with

$$H_k = \left\{\left[R_k\left(1-u_k^2\right)^{1/2}F_{1k} - r_k F_{2k}\right] + F_k\frac{1}{R_k\left(1-u_k^2\right)^{1/2}}\right\}, \quad (9)$$

$$F_{1k} = \int_0^{2\pi}\frac{\cos\phi}{\left[R_k^2 + r_k^2 - 2r_k R_k\left(1-u_k^2\right)^{1/2}\cos\phi\right]^{3/2}}\mathrm{d}\phi\ , \quad (10)$$

$$F_{2k} = \int_0^{2\pi}\frac{(\cos\phi)^2}{\left[R_k^2 + r_k^2 - 2r_k R_k\left(1-u_k^2\right)^{1/2}\cos\phi\right]^{3/2}}\mathrm{d}\phi \quad (11)$$

and

$$u_k = \cos\theta_k\ . \quad (12)$$

Here θ_k represents the polar angle associated with the k-th loop, as illustrated in Fig.4b.

Equations (8) through (11) represent the generalization of the integral approach for the calculation of the stimulation field of the slinky geometry. This formulation demands a large computational effort to determine the field gradient distribution, because for each point in space, there are three integrals to be calculated numerically.

The integral formulation can be avoided by use of a spherical harmonics expansion[8] for the inverse of the denominator of (6). In addition, computation is greatly reduced if the field gradient in the x direction is also calculated in closed form. We show in this paper that the field gradient can be cast into the form

$$\frac{dE_x}{dx} = -\frac{\mu_0}{4}\sum_{k=1}^{N}\frac{di_k}{dt}\frac{x\left(y\cos\alpha_k + z\sin\alpha_k - r_k\right)}{R_k^4}G_k\ , \quad (13)$$

with

$$G_k = \begin{cases}\displaystyle\sum_{l=1}^{\infty}a_l\left(\frac{r_k}{R_k}\right)^{2l+2}H_{1k},\ r_k < R_k \\ \displaystyle\sum_{l=1}^{\infty}a_l\left(\frac{R_k}{r_k}\right)^{2l+1}H_{2k},\ r_k > R_k\end{cases}, \quad (14)$$

$$H_{1k} = -(2l+3)R_k P1_{2l+1} + \left(y\sin\alpha_k - z\cos\alpha_k\right)P2_{2l+1} \quad (15)$$

and

$$H_{2k} = 2lR_k P1_{2l+1} + \left(y\sin\alpha_k - z\cos\alpha_k\right)P2_{2l+1} \quad (16)$$

In (15) and (16), the Legendre polynomials derivatives are expressed as combinations of the Legendre polynomials in the form

$$P1_l\left(u_k\right) = \frac{l}{u_k^2 - 1}\left[u_k P_l\left(u_k\right) - P_{l-1}\left(u_k\right)\right], \quad (17)$$

$$P2_l\left(u_k\right) = \frac{l}{\left(u_k^2-1\right)^2}\left\{\begin{matrix}\left[(l-1){u_k}^2 - (l+1)\right]P_l\left(u_k\right) \\ + 2xP_{l-1}\left(u_k\right)\end{matrix}\right\} \quad (18)$$

and the spherical coordinates of the k-th loop are related to the laboratory reference frame by

$$u_k = \frac{-y\sin\alpha_k + z\cos\alpha_k}{R_k} \quad (19)$$

$$R_k = \sqrt{x^2 + y^2 + z^2 + r_k^2 - 2r_k\left(y\cos\alpha_k + z\sin\alpha_k\right)} \quad (20)$$

with α_k representing the tilt angle of the k-th loop and x, y and z the coordinates of a point in space.

V. Discussion

We have implemented a Mathcad 2001 code to calculate both the E-field distribution and Field gradient for both the integral and Legendre expansion formulations. The Built-in integral calculator and Legendre functions within Mathcad were used in the computation. For the case of the Legendre expansion approach, the series expansion for both field and field derivative were truncated when the result was precise within 0.1%. This was the same tolerance used for the numerical integral evaluation within Mathcad. We noticed that the Legendre expansion approach was much faster than the integral formulation approach and this was even more pronounced as the number of loops increased. In fact, for a large number of loops (> 10), the integral formulation becomes computationally unfeasible.

We noticed a drawback in using the Legendre expansion formulation, in which each term of the E-field expansion, although being a continuous function, had a discontinuous derivative for the k-th loop when the distance of the loop center to a point in space equals the loop radius. Obviously, if all terms in the sum were included in the sum this would not be a problem. However, when a truncation is done, the E-field derivative becomes discontinuous at this condition. For the case with all loops lying in the upper hemisphere and the axon is placed parallel to the x direction on the y=0 surface and for negative z, this is not a problem. This discontinuity problem can be overcome by first differentiating (5) with respect with the x coordinate and then carrying out the spherical harmonics expansion. This development is underway.

VI. CONCLUSIONS

We have developed a computationally efficient method to calculate the field gradient distribution of a generalized slinky coil. These results are currently being used to the simulation of impulse propagation in peripheral nerves and for studies of coil design optimization based on these numerical simulations. Real time behavior of the nerve cell dynamics is under study and those will be reported elsewhere as results become available.

REFERENCES

[1] A. T. Barker, R. Jalinous. e I. Freeston, "Non-invasive magnetic stimulation of the human motor cortex", *Lancet*, vol. 1, pp. 1106-1107 (1985).

[2] M. George, E. M. Wassermann and R. M. Prost, "Transcranial magnetic stimulation: a neuropsychiatric tool for the 21st century", *Journal of Neuropsychiatric and Clinical Neurosciences*, vol. 8, pp.373-382, 1996.

[3] A. L. Hodgkin and A. F. Huxley, "A quantitative description of membrane current and its application to conduction and excitation in nerve", *Journal of Physiology*, no. 117, pp.500-544, 1952.

[4] J. Malmivuo, R. Plonsey, “Bioelectromagnetism: principles and applications of bioelectric and biomagnetic fields”, *Oxford University*, Oxford, 1995.

[5] Kai-Hsiung Hsu, Srikantan S. Nagarajan, and Dominique M. Durand, “Analysis of Efficiency of Magnetic Stimulation,” IEEE Transactions on Biomedical Engineering, vol.50, no. 11, pp. 1276-1285, Nov. 2003.

[6] C. Ren, P. P. Tarjan, and D. B. Popovic, “ A Novel Electric Design for Electromagnetic Stimulation – The Slinky Coil,” IEEE Transactions on Biomedical Engineering, vol. 42, no. 9, pp. 918-925, Sep. 1995.

[7] M. A. F. Feitosa and Eduardo Fontana, “Prospects for the Development of a Magnetic Stimulation Device for Human Tissue,” Proceedings of the 2005 International Microwave and Optoelectronics Conference. Brasília 2005. v. 1. p. 1-4.

[8] J. D. Jackson, “Classical Electrodynamics,” 3rd edition, Wiley, 1999.